An Approach to Turbulent Incompressible Separation under Adverse Pressure Gradients

FABIO R. GOLDSCHMIED*
Sperry Utah Company,† Salt Lake City, Utah

A separation criterion is developed, relating the maximum pressure-recovery ratio at separation to the skin-friction coefficient at the start of the adverse gradient. This criterion shows very good agreement with six experimental points. A method of computing the skin friction is also given, and it has been applied to three experimental runs; the agreement is good in two cases and poor in the third. The present theory indicates that separation will move upstream with increasing Reynolds number, therefore affecting the scaling procedures from model test to prototypes. The theory also indicates that inviscid pressure profiles must be considered in relation to the desired operational Reynolds number, since the effective pressure gradients and the pressure-recovery ratios will change. The theory is based on the assumptions of dissipative-region similarity under any pressure gradient and of a constant total-head line at a fixed distance from the wall under adverse pressure gradients.

Nomenclature

x = streamwise distance
x_s = streamwise separation distance
x_1 = point of minimum pressure and start of adverse pressure gradient
x_0 = equivalent reference length
y = distance from the wall
y_c = distance of assumed constant total-head line
δ_0 = boundary-layer thickness at x_1
δ_c = thickness of laminar sublayer
θ = momentum thickness
θ_0 = momentum thickness at x_1
L = body length
c = airfoil chord
U = velocity outside boundary layer at x
U_M = velocity outside boundary layer at x_1
U_0 = freestream velocity
u, $\bar{u}$ = mean x velocity within boundary layer
v, $\bar{v}$ = mean y velocity within boundary layer
u_c = mean x velocity within boundary layer at $y = y_c$
u_s = mean x velocity within boundary layer at y_c, x_s
u^* = frictional velocity
$u_0{}^*$ = frictional velocity at x_1
$u_s{}^*$ = frictional velocity at x_s
p = static pressure (assumed constant across boundary layer)
p_m = static pressure at x_1
p_s = static pressure at x_s
h = total pressure
h_c = total pressure at y_c
τ = skin friction
τ_0 = skin friction at x_1
H = δ^*/θ = profile form parameter
C_f = $\tau/\frac{1}{2}\rho U^2$ = skin-friction coefficient
C_{f_0} = $\tau_0/\frac{1}{2}\rho U_M{}^2$ = skin-friction coefficient at x_1
C_p = pressure coefficient
C_{p_s} = pressure coefficient at x_s
R_0 = $x_0 U_M/\nu$ = friction equivalent flat-plate Reynolds number
ρ = fluid mass density
ν = fluid kinematic viscosity

Presented as Preprint 64-465 at the 1st AIAA Annual Meeting, Washington, D. C., June 29–July 2, 1964; revision received November 18, 1964.

† A division of Sperry Rand Corporation.

* Research Aerodynamicist, Advanced Systems Department.

I. Introduction

THE problem of turbulent flow separation has been and still remains the fundamental problem of hydrodynamics. The prediction of turbulent separation would allow the calculation of the actual pressure distribution on a hydrofoil or on a submerged body and therefore allow the prediction of actual hydrodynamic forces and moments. Furthermore, scale effects between models and prototypes can be accurately assessed only through an understanding of the phenomenon of separation.

Furthermore, little is known as yet about the inverse problem, i.e., the problem of designing the most suitable adverse pressure gradient for maximum lift/drag ratio of hydrofoils or for minimum drag of submerged bodies of maximum displacement.

The adverse pressure gradient may be chosen to be of linear, concave, or convex profile or it may be chosen to be step-wise discontinuous, as with the Griffith-type pressure distribution, where boundary-layer control is required to actually achieve the pressure recovery. There are several methods available for the calculation of the incompressible turbulent boundary layer under adverse pressure gradients, all rather laborious for practical usage by the hydrodynamic designer. Generally, these methods employ the momentum integral equation, with auxiliary equations for the skin friction and for the profile form parameter H. The parameter H is usually taken as a gross index of separation.

Thwaites[1] gives an excellent discussion of such methods which need not be repeated here. Stewart[2] has reviewed six such methods and tested them against the experimental results of Von Doenhoff and Tetervin,[3] Schubauer and Klebanoff,[4] and of Clauser.[5]‡ It is seen that all the methods fail against the results of the Clauser pressure distribution no. 2. The method of Truckenbrodt[6] appears the most suitable for engineering usage, and it also provides the least poor agreement, among all methods, with the Clauser results.

Having attained the momentum thickness θ and the form parameter H, it is possible to employ the Ludwieg-Tillman[7] equation to obtain the skin friction and also to estimate the separation point by extrapolating the computed skin-friction curve to zero (provided, of course, that θ and H values are computed correctly).

‡ Note: These results are referred to later in this paper as data sets I, II, and IV of Table 1.

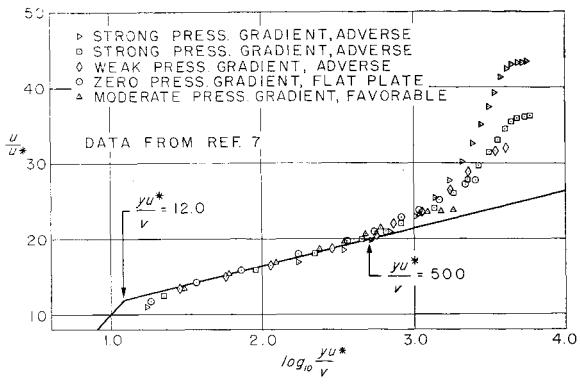

Fig. 1 Friction velocity ratio vs friction distance parameter for several pressure gradients; u/u^* vs $\log_{10} yu^*/\nu$.

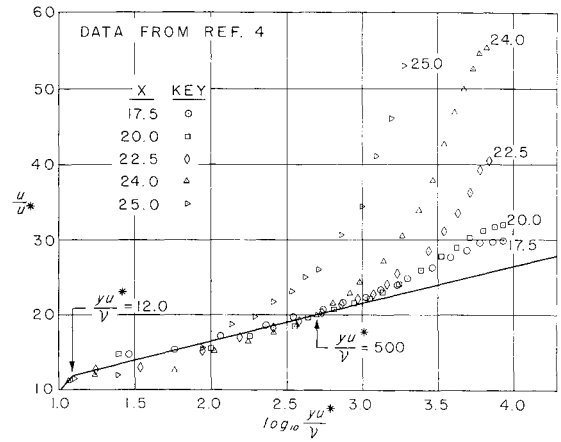

Fig. 2 Friction velocity ratio vs friction distance parameter for adverse pressure gradient up to separation; u/u^* vs $\log_{10} yu^*/\nu$.

It would be possible to conclude that the forementioned methods were adequate if it were not for the evidence of the so-called "equilibrium" boundary layers of Clauser and Stratford,[8] where H flattens out rather than increasing sharply. The equilibrium boundary layers, produced by a particularly concave pressure distribution, will run with profile similarity despite the adverse gradient. Whether such boundary layer will or will not separate eventually, the allowable pressure recovery is finite because of the shape of the pressure distribution becoming asymptotic.

II. Analysis

A. General

The present analysis is based on two physical observations regarding conditions within an incompressible two-dimensional turbulent boundary layer under adverse pressure gradients. Both observations are directly verified by experimental evidence. The conclusions concerning prediction of the separation pressure-recovery ratio and of the skin-friction trend are verified against five experimental runs.

B. Dissipative Region Similarity

The first observation pertains to the so-called dissipative region within the boundary layer. According to the energy analysis presented by Townsend,[9] the turbulent boundary layer may be divided into the following regions, on the basis of energy flow considerations:

1) In the mixing region, or outer portion, the energy flow from the freestream is captured, so to speak, by a cylindrical vortex. For instance, the function of the so-called vortex generators, is to strengthen these cylindrical vortices and increase the energy interchange.

2) In the energy transfer region, or the middle portion, the energy flow of turbulent energy production $\tau(\partial\bar{u}/\partial y)$ is directed toward the wall.

3) In the dissipative region or in the inner portion that includes the laminar sublayer, all the energy flow is absorbed and dissipated.

In the dissipative region the energy absorption must occur at such high rates that dissipation will be the predominant characteristic, and therefore there will be similarity of the velocity profiles on the basis of some dissipation parameter.

It should be noted again that similarity should always be expected only in the dissipative region close to the wall and not in the rest of the boundary layer. Only in the special case of equilibrium boundary layers, as demonstrated by Clauser[5] and Stratford,[8] can similarity be expected for the complete boundary layer under adverse pressure gradients. Experimental proof of dissipative-region similarity is given by Ludwieg and Tillman[7] and by Schubauer and Klebanoff.[4] Data from boundary-layer profiles ranging from flat plate to separation are plotted together in the Karman logarithmic manner, i.e., u/u^* vs $\log_{10}(yu^*/\nu)$, and are shown in Fig. 1 (from Ref. 7) and in Fig. 2 (from Ref. 4).

It is seen that, up to $u/u^* = 20$ and up to $yu^*/\nu = 500$, all data points fall on one universal curve, regardless of pressure gradient, up to separation. In Fig. 2 the velocity profile begins deviating at $yu^*/\nu = 100$ for the $x = 25.0$-ft station. Since separation is observed at $x = 25.4$ ft, the profile deviation can well be expected at $x = 25.0$ ft.

However, even this deviation will not affect the analysis, as will be discussed in the next section, because the yu^*/ν values of interest near separation will be much less than 100 and actually of the order of 10. The values of u^* employed in plotting the profiles of Fig. 2 are not the hot-wire experimental skin-friction data of Schubauer and Klebanoff[4] but are somewhat lower and are shown in Fig. 3.

As is generally agreed, the hot-wire data are considerably too high, at least by a factor of 1.25. At the 17.5-ft station (start of pressure gradient), the hot-wire skin-friction value should agree with the conventional flat-plate formulas, such as Falkner's,[10] Schulz-Grunow's,[11] etc. An experimental method for the determination of the skin friction may be derived from the forementioned conclusions; it would be sufficient to measure the velocity at some five points within the dissipative region and then find by trial and error the value of u^* for which the points best fit the universal curve. A small wall-mounted fixed rake would be a suitable tool for this method. If the y value is fixed, as will be discussed later, yu^*/ν will always decrease when going downstream against a pressure-gradient because u^* will always decrease; i.e., if the initial y point falls within the dissipative region, all downstream points at constant y will also fall within this region.

The evidence for the dissipative region similarity up to separation is generally accepted, having been recognized in

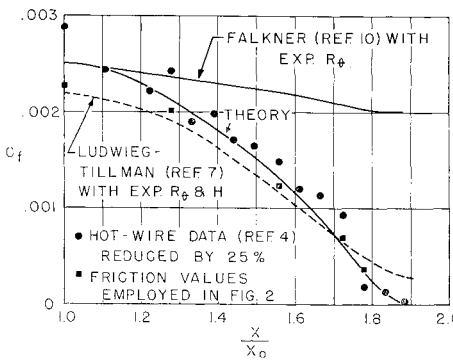

Fig. 3 Skin friction vs normalized streamwise distance, C_f vs x/x_0

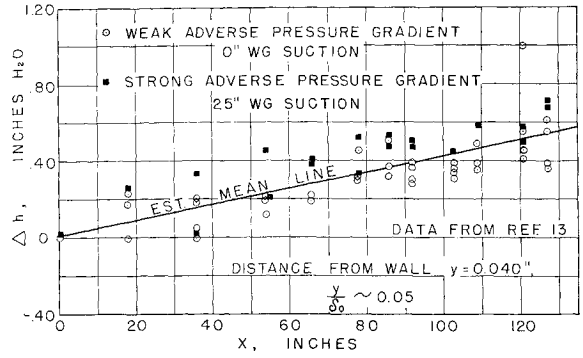

Fig. 4 Total-head difference vs streamwise distance at constant y distance from the wall; Δh vs x.

the past by several workers (Goldschmied,[12] Clauser,[5] etc.). Unfortunately, Clauser, although recognizing the similarity (as shown in his Fig. 4) and exploiting it for the determination of the skin-friction law for equilibrium boundary layers, fails to display the data for his own equilibrium profiles.

C. Constant Total-Head Line

The second observation pertains to the trend of total head at fixed y distances from the wall, within a turbulent boundary layer under adverse pressure gradients. It is well known that the total head remains constant in the freestream at very large y distances from the wall. At the wall itself, the static pressure increases by definition (adverse pressure gradient). It has long been recognized that, within the boundary layer at comparatively large y distances from the wall, the total head decreases. In fact, on a flat plate with zero gradients, the total head decreases at all $y > 0$ distances.

However, what is not generally recognized is that under adverse pressure gradients, at small y distances from the wall, the total head definitely increases, which means that excess energy is being supplied to the fluid layer. However strange this notion may seem at first, it is in agreement with the concept of the dissipative layer receiving the energy flow transferred down from the energy transfer region. Some experimental evidence seems to indicate that such increasing total-head lines are independent of pressure gradient, at least when the adverse pressure gradient is not too high. Figure 4 shows the total head Δh against streamwise distance x for both a weak and a strong pressure gradient, as a distance

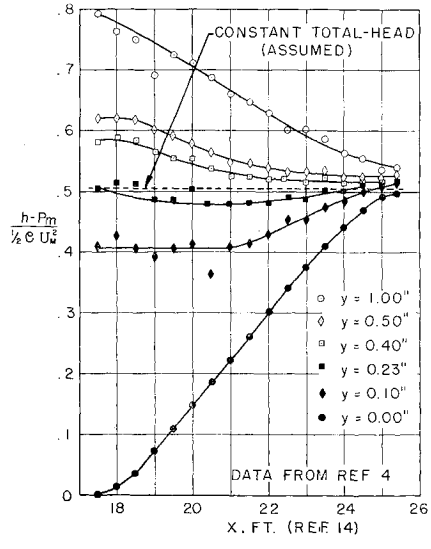

Fig. 5 Total-head coefficient vs streamwise distance at constant y distances from the wall; $h-p_m/\frac{1}{2}\rho U_M^2$ vs x.

$y = 0.040$ in. or $y/\delta_0 = 0.05$ (where δ_0 is the initial boundary-layer thickness). It is seen that both trends are practically the same. The adverse pressure gradient starts at $x = 0$. Figure 4 is plotted from some unpublished NACA data by Goldschmied.[13] Figure 5 shows a complete plot of $(h - p_m)/\frac{1}{2}\rho U_M^2$ vs x at constant y from the data of Schubauer and Klebanoff.[4] It is seen that there are lines of decreasing total-head parameter for $y = 1.00$ in., $y = 0.50$ in., and $y = 0.40$ in. and lines of increasing total-head parameter for $y = 0$ and $y = 0.10$ in. At $y = 0.23$ in. there is a linear of substantially constant total head, bounded by the increasing trends and by the decreasing trends. Figure 6 shows a comparable plot for what is claimed to be the extreme pressure-gradient case, namely, the zero-friction equilibrium experiment of Stratford.[8]

It is seen that there are trends at constant y distance that are both decreasing and then increasing, thus indicating that there cannot be a line of substantially constant total head, although there is a line with the same total-head value at the beginning and at the end. If useful results can be achieved, it is permissible to make the simple assumption, as suggested by Goldschmied,[12] that there is, in all cases, a line at constant y with exactly constant total head. If this line exists, it should be somewhere in the dissipative region and therefore it will be assumed to be independent of pressure distribution (although it has been seen that it is not always true).

If the boundary layer is known initially at the point of minimum pressure, the problem arises of determining the total-head value of this assumed constant total-head line and its y distance from the wall. The outer edge of the dissipative region will be a reasonable choice as the starting point of this line; it is to be noted that if the total head of the edge of the dissipative region is plotted against streamwise distance, a minimum will be shown at the point at minimum static pressure, because it decreases under favorable gradients and it increases under adverse gradients. A quantitative analysis may then be attempted, to be applied to five different sets of experimental data for critical demonstration of the results.

From Figs. 1 and 2, the outer edge of the dissipative region is characterized approximately by $u/u^* = 20$ and $yu^*/\nu = 500$. Therefore, the total head will be $h_e = \frac{1}{2}\rho(20u_0^*)^2 + p_m$. The distance from the wall will be given by $y_e = 500\nu/u_0^*$.

D. Determination of Skin Friction

At some downstream station (at $y = y_e$), $h = h_e$ and the velocity u_e may be found as follows:

$$p_m + \tfrac{1}{2}\rho(20u_0^*)^2 = p + \tfrac{1}{2}\rho u_e^2$$

$$p_m - p + \tfrac{1}{2}\rho 400\,\frac{\tau_0}{\rho} = \tfrac{1}{2}\rho u_e^2$$

$$\left(\frac{u_e}{U_M}\right)^2 = \frac{p_m - p}{\frac{1}{2}\rho U_M^2} + 400\,\frac{\tau_0}{\rho U_M^2}$$

Noting that

$$C_{f_0} = \frac{\tau_0}{\frac{1}{2}\rho U_M^2}$$

then

$$\frac{u_e}{U_M} = \left[400\,\frac{C_{f_0}}{2} - \frac{p - p_m}{\frac{1}{2}\rho U_M^2}\right]^{1/2}$$

Noting that

$$C_p = \frac{p - p_m}{\frac{1}{2}\rho U_M^2} = 1 - \left(\frac{U}{U_M}\right)^2$$

it can be written

$$\frac{u_e}{U_M} = [200\,C_{f_0} - C_p]^{1/2}$$

Now C_p is known from the pressure distribution, obtained experimentally or theoretically. If U_M, C_{pm}, and p_m represent the velocity, pressure coefficient, and pressure, respectively, at the point of minimum pressure

$$C_p = 1 - (V/V_M)^2$$

where

$$V = U/U_0 \qquad V_M = U_M/U_0$$

and U_0 is the freestream or flight velocity. Thus when u and $y = y_c$ are known, the skin-friction coefficient c_f may be found as follows. Take

$$G = U/U_M[C_f/C_{f_0}]^{1/2}$$

and

$$K = u_c/u^*$$

Then

$$K = \frac{[400 - 2(C_p/C_{f0})]^{1/2}}{G}$$

On the other hand,

$$K = A + B \log_{10}(y_c u^*/\nu)$$

and

$$y_c/\nu = 500/u_0^*$$

From Figs. 1 and 2, $A = 6.67$, $B = 4.93$, and substituting for G, therefore,

$$K = 6.67 + 4.93 \log_{10}[500G]$$

The two equations for G may be solved graphically and the G value determined for each C_p and for a known initial skin-friction coefficient C_{f_0}:

$$\frac{[400 - 2(C_p/C_{f_0})]^{1/2}}{G} = 6.67 + 4.93 \log_{10}[500G]$$

and

$$C_f = C_{f_0} G^2 (U_M/U)$$

Figure 7 shows C_f plotted against C_p for several values of C_{f_0}.

It is to be noted that the curves of Fig. 7 are based on the previous assumptions that the total head is exactly constant at $y = y_c$. It has been already seen that this assumption agrees well with the data of Schubauer and Klebanoff but it agrees only poorly with the data of Stratford.

E. Turbulent Separation Criterion

To establish a turbulent separation criterion, the hypothesis is made that separation occurs (for the purposes of the present theory) when the assumed constant total-head line reaches the edge of the laminar sublayer.

If the Reynolds equation is written at the line of constant total head, by definition,

$$\frac{\partial}{\partial x}\left(\frac{u_c^2}{2} + \frac{p}{\rho}\right) = 0$$

Therefore,

$$\nu \frac{\partial u}{\partial y} = \frac{\partial}{\partial y}\left(\nu \frac{\partial u}{\partial y}\right) + \frac{\partial}{\partial y}(-\overline{u'v'})$$

whereas at the wall itself

$$\frac{\partial}{\partial y}\left(\nu \frac{\partial u}{\partial y}\right) = \frac{1}{\rho}\frac{\partial p}{\partial x}$$

At the separation point, it is assumed that $y_c = \delta_l$. Although the velocity profile within the sublayer under adverse pressure gradient cannot be exactly linear because of the foremention wall condition, it has been found experimentally that the velocity profile is substantially linear. Perhaps this is so because the velocity gradient induced by $\partial p/\partial x$ occurs only locally at the very wall. Figures 1 and 2 show similarity for all profiles at the edge of the sublayer. Thus at $y_c = \delta_l$ corresponding to $y_c u^*/\nu = 12$

$$(\partial/\partial y)[\nu(\partial u/\partial y)] = 0$$

Furthermore, it is known that the shear correlation vanishes near the sublayer, $(-\overline{u'v'}) \cong 0$. It must follow that

$$\frac{\partial u}{\partial y}\int_0^{\delta_l} \frac{\partial u}{\partial x}\, dy = 0$$

However, since the integral cannot go to zero because the function is finite, at least at the upper limit $\partial u/\partial y$ must go to zero. The fact that $\partial u/\partial y$ becomes zero satisfies the conventional definition of separation. Separation should then ensue when the assumed constant total-head line reaches the laminar sublayer.

In the laminar sublayer, as suggested by von Karman, $u/u^* = yu^*/\nu$. In the dissipative region

$$u/u^* = 6.67 + 4.93 \log_{10}(yu^*/\nu)$$

The limit of the laminar sublayer is obtained at the intersection of the two equations at

$$u/u^* = yu^*/\nu = 12$$

At the point of minimum pressure (start of the adverse gradient), $y_c u_0^*/\nu = 500$. At the point of separation $y_c u_s^*/\nu = 12$. Therefore, $u_s^*/u_0^* = 12/500 = 1/41.5$.

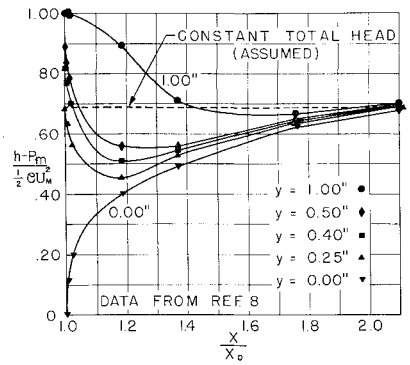

Fig. 6 Total-head coefficient vs normalized streamwise distance at constant y distances from the wall; $h - p_m/\frac{1}{2}eV_M^2$ vs x/x_0.

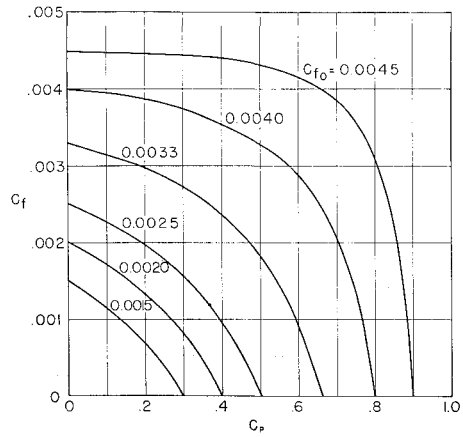

Fig. 7 Theoretical local skin-friction coefficient vs static pressure coefficient.

Table 1 Five sets of experimental data

Data set	Ref.	Date	Test run
I	3	1943	NACA 65(216)222 airfoil at $\alpha = 10.1°$
II	4	1950	Main test
III	16	1953	25 in. WG suction
IV	5	1954	Pressure distribution no. 2
V	8	1959	Main test

Since

$$u_0^* = U_M \left[\frac{C_{f_0}}{2}\right]^{1/2}$$

then separation is assumed to take place when

$$u_s^* = U\left[\frac{C_f}{2}\right]^{1/2} = \frac{U_M}{41.5}\left[\frac{C_{f_0}}{2}\right]^{1/2}$$

and the corresponding separation velocity u_s at $y = y_c$;

$$u_s = 12u_s^* = \frac{12}{41.5}\,U_M\left[\frac{C_{f_0}}{2}\right]^{1/2} = \frac{U_M}{3.45}\left[\frac{C_{f_0}}{2}\right]^{1/2}$$

But

$$u_c/U_M = [200C_{f_0} - C_p]^{1/2}$$

Therefore,

$$\frac{u_s}{U_M} = \frac{1}{3.45}\left[\frac{C_{f_0}}{2}\right]^{1/2} = \left[400\,\frac{C_{f_0}}{2} - C_{p_s}\right]^{1/2}$$

$$C_{f_0}/23.8 = 200\,C_{f_0} - C_{p_s}$$

$$C_{p_s} = (p_s - p_m)/\tfrac{1}{2}\rho U_M^2 = C_{f_0}(200 - 0.042)$$

$$C_{p_s} \equiv 200C_{f_0}$$

The foregoing equation becomes the separation criterion of the present theory.

The first question is whether C_{p_s} becomes equal to or larger than 1.0 (physically impossible) for the highest value of C_{f_0} which is achievable for turbulent boundary layers. Dhawan[14] shows $C_f = 0.0044$ as the highest experimental value, whereas Smith and Walker[15] show $C_f = 0.00375$ and extrapolate to $C_f = 0.0045$. From other sources, $R_\theta = 500$ is believed to be the minimum possible for a turbulent boundary layer; $C_f = 0.00435$ should correspond to $R_\theta = 500$. Thus the maximum possible pressure recovery ratio C_{p_s} at separation cannot exceed 0.87 or 0.88.

III. Experimental Verification

A. General

Experimental verification of a turbulent separation criterion is a difficult task, because a wide range of experimental data would be required, regarding both pressure-gradients and Reynolds number. In particular, for the present theory it is required to identify carefully the starting point of the turbulent boundary layer into the adverse pressure gradient in regard to both local skin-friction coefficient C_{f_0} and pressure parameter C_{p_m}.

Unfortunately many authors omit this information in direct form, and therefore it must be deduced more or less accurately from related data. Five sets of experimental data have been chosen for verification of the theory, as shown in Table 1. It is to be noted that the skin friction is given completely only in data sets II and III. For the equilibrium layers IV and V separation is not indicated by the authors, although it is most probable that it did occur somewhere downstream; however, since such pressure distributions become ever flatter streamwise, it is easy to estimate the maximum pressure-recovery ratio achievable.

Table 2 Data summary

Data set	C_{f_0}	$R_0 \times 10^6$	C_{p_s}	X_0, ft	X_0/c
I	0.00267	6	0.495	...	1.4
II	0.0025	9	0.528	9.0	...
III	0.00315	2.3	0.620	6.9	...
IV	0.0040	5	0.826	1.93	...
V	0.0035	1	0.682	3.0	...

B. Data Reduction

As suggested by the present theory, the several pressure distributions will be plotted in the form C_p/C_{f_0} vs x/x_0. The normalizing length x_0 is defined as the equivalent length of flat-plate run at velocity U_M, which is required to produce a local skin-friction coefficient equal to the actual C_{f_0} of the test. At separation, C_{p_s}/C_{f_0} should always be in the vicinity of 200.

Data set I

Airfoil Reynolds number

$$R = U_0 c/\nu = 2.64 \times 10^6$$

At starting point

$$\theta_0/c = 0.55 \times 10^{-3} \qquad U_0\theta_0/\nu = 1.45 \times 10^3$$

$$U_M/U_0 = 1.62 \qquad U_s/U_0 = 1.15 \qquad \text{(separation clearly indicated)}$$

$$U_M\theta_0/\nu = R_\theta = 1.45 \times 1.62 \times 10^3 = 2.35 \times 10^3$$

The form parameter $H_0 = 1.565$ at the starting point. Using the Ludwieg-Tillman[7] skin-friction equation, since this is not a flat-plate boundary layer,

$$C_{f_0} = 0.246/10^{0.6780}R_\theta^{0.268H_0} = 0.00267$$

The separation pressure-recovery ratio will be

$$C_{p_s} = 1 - \frac{V_s^2}{V_M^2} = 1 - \frac{1.15^2}{1.62^2} = 1 - 0.505$$

$$C_{p_s} = 0.495$$

For the calculated C_{f_0}, the equivalent flat-plate Reynolds number will be

$$R_0 = x_0 U_M/\nu = 6 \times 10^6$$

The airfoil Reynolds number is

$$R = U_M C/\nu = 2.64 \times 1.62 \times 10^6 = 4.28 \times 10^6$$

Thus

$$x_0/C = 6 \times 10^6/4.28 \times 10^6 = 1.4$$

Data set II

The initial skin friction must be between $C_{f_0} = 0.0022$ and $C_{f_0} = 0.0025$. The low limit is given by the Ludwieg-Tillman formula and the high limit is given by the Falkner formula. The hot-wire experimental points, when reduced by 25%, agree with the high limit. The value $C_{f_0} = 0.0025$ was chosen as more probable, requiring an equivalent flat-plate Reynolds number $R_0 = 9 \times 10^6$. Separation is clearly indicated by the authors, i.e., $C_{p_s} = 0.528$. The velocity $U_M = 160$ fps; thus

$$x_0 160/\nu = 9 \times 10^6 \qquad x_0 = 9 \text{ ft}$$

Data set III

The heat-transfer skin-friction data and the Ludwieg-Tillman equation define $C_{f_0} = 0.00315$ to a reasonable accuracy. The equivalent flat-plate Reynolds number will be

$$R_0 = 2.3 \times 10^6$$

Since at the initial point

$$R = 3.33 \times 10^5/\text{ft}$$

$$x_0 = 2.3 \times 10^6/3.33 \times 10^5 = 6.9 \text{ ft}$$

The separation point is well defined by the author; thus $C_{p_s} = 0.620$.

Data set IV

It is difficult to interpret Clauser's paper for the purposes of the present theory. The starting point is taken at $x = 15$ in., since there is a trip wire presumably at $x = 0$. The initial skin friction is determined by extrapolating the upper curve of Clauser's Fig. 9 (calculated constant pressure curve) to $x = 15$ in.; it is presumed that C_{f_0} should correspond to the flat-plate value. Thus, $C_{f_0} = 0.004$ and the corresponding equivalent flat-plate Reynolds number is $R_0 = 5 \times 10^5$. From Clauser's Fig. 6 the velocity is taken at $x = 15$ in., $U_M = 40.2$ fps, thus yielding $x_0 = 1.93$ ft. It is to be noted that nowhere in Clauser's paper does there appear a test Reynolds number value. From $C_{f_0} = 0.004$ it would appear that the corresponding flat plate $R_\theta = 787$, i.e., just about high enough to guarantee the boundary layer to be turbulent. No mention is made by the author of separation, following the equilibrium run. However, it is estimated that the maximum pressure-recovery ratio should be between $C_{p_s} = 0.826$ and $C_{p_s} = 0.837$. In fact the last equilibrium profile presented is at $x = 230$ in. or $C_p = 0.740$, and furthermore the skin friction begins to drop at $x = 320$ in. or $C_p = 0.790$.

Data set V

Stratford's initial point is clearly defined and the equivalent flat-plate Reynolds number is stated to be $R_0 = 1 \times 10^6$, together with $x_0 = 3$ ft. In accordance with R_0, $C_{f_0} = 0.0035$. No mention is made by the author of separation, but it is quite probable that separation may be placed no later than $C_p = 0.682$. For convenience, the experimental data are tabulated in Table 2.

C. Turbulent Separation Criterion

The pressure gradients of the five experimental references are shown in Fig. 8, plotted in the manner C_p/C_{f_0} vs x/x_0. This normalizing method is suggested by the present theory, and it serves to illustrate the comparative strength of the several gradients. It is to be noted that x_0 is not defined in the same way as is Stratford's. The final (separation) point of the curves shows the maximum pressure-recovery achieved. It is seen that C_p/C_{f_0} varies from 183 to 210, whereas the theoretical predicted value is 200. The gradients may be classified in a rough empirical fashion by the x/x_0 values, where C_p/C_{f_0} equals 50% and 90% of the final value.

The pressure gradients are summarized in Table 3 for visual inspection. It is seen that Stratford's equilibrium gradient is the strongest at the 50% point, whereas Clauser's equilibrium gradient is the weakest. It may be noted that Stratford's gradient has the general shape of the wall pressure of a turbulent boundary layer under a normal shock wave. Clauser's gradient appears to be very weak because the initial Reynolds number is very low and x_0 is small; it is seen how the pressure-recovery capability of the boundary layer is taken into account into the streamwise length normalization. Figure 9 shows C_{f_0} vs C_{p_s}; there is good agreement for all five experimental references, ranging from $C_{p_s} = 0.50$ to $C_{p_s} = 0.826$, as well as for an additional separation point obtained by Newman[17] and quoted by Robertson.[18]

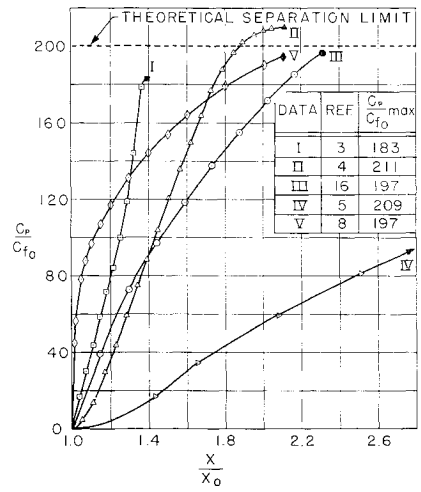

Fig. 8 Normalized pressure gradients C_p/C_{f_0} vs x/x_0.

It is well known that the customary H criterion for separation would fail for both equilibrium cases (IV and V). It is to be repeated here that the present theory predicts the maximum pressure-recovery ratio achievable, not a local profile-form parameter or a local pressure-gradient parameter for separation.

At this point a useful comparison may be made with the Robertson[18] separation theory, because it also arrives at C_{f_0} as the separation parameter. The mean Robertson theoretical curve, as taken from Fig. 2 of Ref. 18, is shown in Fig. 9; it is seen that its trend is opposite to the experimental evidence and to the present theory.

In addition, in Fig. 9 are plotted four supersonic points at Mach numbers of 2 and 3 to demonstrate the case of very low pressure recoveries and skin-friction values, taken from the work of Donaldson and Lange.[19]

It is to be noted that the separation criterion of the present theory seems to be well verified by a range of experimental data despite the simplified assumption of an exactly constant total-head line.

It appears from these results that, since the maximum pressure-recovery depends only on the initial skin friction C_{f_0}, the strongest gradient may be employed to reduce the streamwise length required for such pressure recovery. As a crude approximation, it may be said, considering curve I of Fig. 8, that a length $(x - x_0)/x_0 = 0.4$ can be a minimum required to produce $C_{p_s} = 200\ C_{f_0}$. This rule can assist the hydrodynamic designer in selecting the pressure distribution shape of

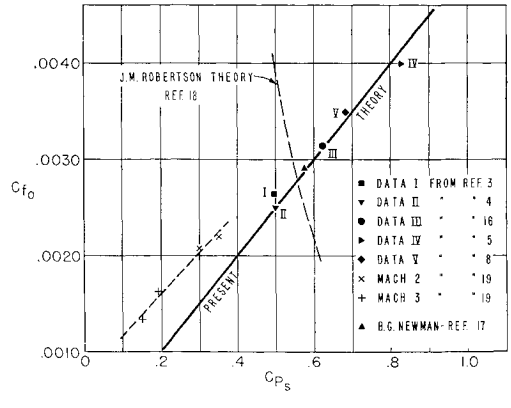

Fig. 9 Turbulent separation criterion: initial local skin-friction coefficient vs maximum pressure recovery at separation, C_{f_0} vs C_{p_s}.

hydrofoils and submerged bodies for any particular Reynolds number of operation. If, however, less than C_{p_s} is required, then the curve V should be followed, up to $C_p/C_{f_0} = 130$, to provide the shortest streamwise length.

As an illustration of this approach, a 3:1 fineness-ratio submerged body will be considered, designed to have a Griffith-type step-pressure distribution, with the pressure discontinuity at 85% length. The over-all pressure-recovery ratio required is $C_p = 0.64$, from 85% length to the tail; typically a suction boundary-layer control slot is employed to enable the pressure jump to be negotiated without separation. However, if C_{f_0} at 85% length can be equal to, or greater than, 0.0032, then some pressure distribution (as in Fig. 8) may be employed to negotiate the same pressure-recovery without boundary-layer control; however, it is found that

$$x_0/L = 2 \times 10^6/R_L \text{ for } C_{f_0} = 0.0032$$

where $R_L = U_0 L/\nu$, and $R_L = 1.3 \times 10^6$ to provide $C_{f_0} = 0.0032$ with transition at 10% length. Thus $x_0/L = 1.54$. Taking $(x - x_0)/x_0 = 0.4$ (as for curve I of Fig. 8) as the shortest streamwise distance, then $(x - x_0)/x_0 = \Delta x/L = 0.615$. This means that although $\Delta x/L = 0.15$ is available for pressure recovery, $\Delta x/L = 0.615$ is required as a minimum. Furthermore, the maximum body Reynolds number is $R_L = 1.3 \times 10^6$ so as to provide the required initial skin friction for avoidance of separation. This example illustrates the usefulness of the present theory for hydrodynamic design as a function of Reynolds number or inversely for extrapolating model test results to prototype's.

D. Skin Friction

The skin-friction coefficients under adverse pressure gradients are completely given in data sets II and III, measured by hot-wire and wall-type heat-transfer instruments, respectively. The hot-wire data have been reduced by 25% so as to obtain agreement with conventional data at the starting point. The initial skin-friction values are well defined. From data set IV, however, there are obtained data only for a partial test length from $x/x_0 = 3.65$ to $x/x_0 = 14.4$; the initial skin-friction value is obtained from the flat-plate curve extrapolated to $x = 15$ in., $x/x_0 = 1$. The initial value C_{f_0} is joined to the test data by a faired interpolation.

Figure 10 presents the data from sets II, III, and IV in the normalized form C_f/C_{f_0} vs x/x_0. Figure 3 shows a plot of C_f vs x/x_0 from set II; in addition to the present theory, they are plotted curves for the Ludwieg-Tillman[7] and the Falkner[10] skin-friction formulas, using experimental values for R_θ and H. The present theory is in excellent agreement with the hot-wire data (reduced by 25%); the Ludwieg-Tillman curve is also in good agreement, particularly with the points corresponding to the u^* values used in Fig. 2. The Falkner flat-plate formula, as expected, predicts consistently high skin-friction values. The average true skin friction is seen to be substantially less than the flat-plate average; this clearly undermines the commonly used concept of computing total drag coefficient based on wetted body surface area to be compared with flat-plate values, so as to determine by their difference the amount of pressure (form) drag.

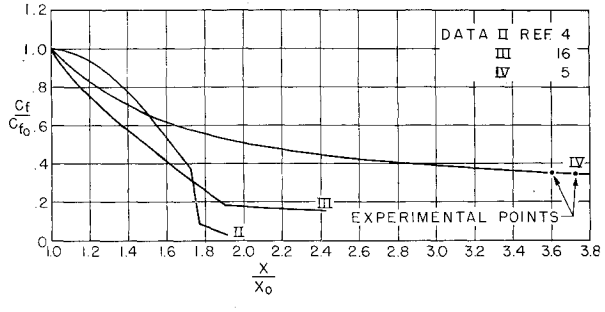

Fig. 10 Skin-friction ratio vs normalized streamwise distance, C_f/C_{f_0} vs x/x_0

In Fig. 3 the Ludwieg-Tillman curve could be used to determine separation approximately by drawing a tangent at the point of inflection at $x/x_0 = 1.78$. Figure 11 shows a plot of C_f vs x/x_0 from set III. It is seen that the present theory is in fair agreement with the heat-transfer data. The Ludwieg-Tillman curve is in better agreement (using experimental R_θ and H values); again it could be used, as it was previously, to determine separation approximately by drawing a tangent to the point of inflexion at $x/x_0 = 2.045$.

Figure 12 shows a plot of C_f vs x/x_0 from set IV. The agreement with the theory is poor; however, the initial point (by definition) and the final point are correct, thus demonstrating at least the right trend. It is clear that the poor agreement is due to the assumption of constant total head at $y = y_c$. Figure 6 from set V demonstrates that the total head can decrease and then increase again; if this were taken into account the agreement would be good. Unfortunately more and better data are needed in order to study the functional relationship of the parameter $(h - p_m)/\frac{1}{2}\rho U_M^2$ at $y = y_c$ with the pressure-gradient distribution and to arrive at an analytical expression.

The computed constant-pressure curve is about 300% higher on the average than the true skin friction; this dramatizes the inadequacy, as pointed out previously, of the concept of total-drag coefficient based on wetted surface area. The Ludwieg-Tillman formula is seen to fail in this case, due to the apparently decreasing trend of H; it cannot be used at all to predict separation.

Finally, it is useful to note that the skin friction obtained from experimental evaluation of the left-hand side of the integral momentum equation yields a rising trend under adverse pressure gradients, as compared to the decreasing trend of the hot-wire and heat-transfer data. This has been discussed in detail by Goldschmied[20] for data set II.

IV. Conclusions

1) The present turbulent separation criterion appears to have adequate experimental verification, including the two cases of equilibrium boundary layers. The H criterion of separation has been shown previously to be invalid by the equilibrium boundary layer with flattening or decreasing H trends. Also the Ludwieg-Tillman skin-friction formula is shown to fail with the equilibrium boundary layer even when applied with experimental values; thus it cannot be relied upon to determine separation by extrapolation. The Stratford separation equation cannot yield any information for the equilibrium pressure gradient at zero skin friction by its very

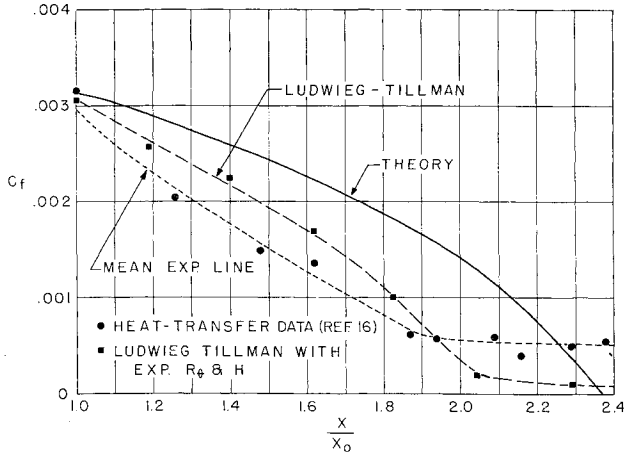

Fig. 11 Skin friction vs normalized streamwise distance, C_f vs x/x_0.

Table 3 Pressure gradients summary

Data set	$\left[\frac{x}{x_0}\right]$ at $\frac{C_p}{C_{f0}} = 50\%$	$\left[\frac{x}{x_0}\right]$ at $\frac{C_p}{C_{f0}} = 90\%$	$\frac{C_{p_s}}{C_{f0}}$
I	1.23	1.35	183
II	1.45	1.80	211
III	1.45	2.07	197
IV	3.05	11.2	209
V	1.10	1.76	195

definition. The simplified assumption of the constant total-head line does not seem to affect the validity of the prediction of the maximum pressure-recovery ratio as a function of initial skin-friction coefficient.

Since the skin friction will decrease with increasing Reynolds number, the maximum pressure recovery will also decrease and pressure-drag losses will increase. This is to be taken into account in the extrapolation of model test data to prototype values through a wide Reynolds number range, such as 10^7 for the model and 10^9 for a submarine prototype. As a consequence of the present separation theory, hydrofoils and submerged bodies may now be analyzed at the proper Reynolds number, taking into account transition location, the particular pressure-distribution profile, and also hull vibration (as it affects the skin friction).

It is to be noted that a calculated inviscid pressure-distribution profile will not be universally suitable for any Reynolds number because of the change of the maximum pressure-recovery ratio. Therefore, such profile must be designed for the desired operational condition.

2) The skin friction computed by the present theory appears to be affected by the simplified assumption of the constant total-head line. The experimental agreement is good for conventional linear gradients but poor with the equilibrium boundary layers. However, even in these cases the theoretical trend is correct.

The Ludwieg-Tillman skin-friction formula shows good agreement with the conventional linear gradients but it fails with the equilibrium boundary layers. Since the turbulent skin friction under adverse pressure gradients is substantially less than the corresponding flat-plate values (even when using the experimental R_θ), dropping to 30%, or less than 10% for the equilibrium cases, the concept of total drag coefficient based on wetted surface area should be abandoned as misleading. Commonly the difference between such a test coefficient and the corresponding average flat-plate value is taken to represent the pressure drag; such procedure may grossly underestimate the pressure drag and furthermore affect even more the extrapolation procedure to higher Reynolds numbers.

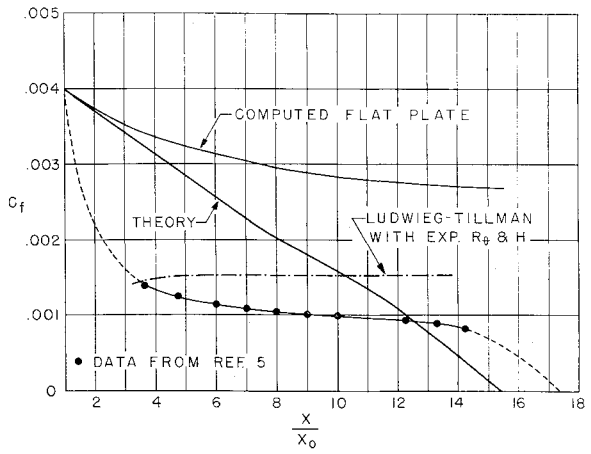

Fig. 12 Skin friction vs normalized streamwise distance, C_f vs x/x_0.

References

[1] Thwaites, B., *Incompressible Aerodynamics* (Oxford Clarendon Press, London, 1960), Chap. II, pp. 67–89.

[2] Stewart, C. C., "A comparison of turbulent boundary-layer theories," Massachusetts Institute of Technology, Gas Turbine Lab. Rept. 57 (March 1960).

[3] Von Doenhoff, A. E. and Tetervin, N., "Determination of general relations for the behavior of turbulent boundary layers," NACA Rept. 772 (1943).

[4] Schubauer, G. B. and Klebanoff, P. S., "Investigation of separation of the turbulent boundary layer," NACA TN 2133 (1950).

[5] Clauser, F. H., "Turbulent boundary-layers in adverse pressure gradients," J. Aeronaut. Sci. **21**, 91–108 (1954).

[6] Truckenbrodt, E., "A method of quadratures for the calculation of the laminar and turbulent boundary-layer in case of plane and rotationally symmetrical flow," NACA TM 1379 (1955).

[7] Ludwieg, H. and Tillman, W., "Investigations of the wall-shearing stress in turbulent boundary layers," NACA TM 1285 (1950).

[8] Stratford, B. S., "An experimental flow with zero skin-friction throughout its region of pressure rise," J. Fluid Mech. **5**, 17–35 (1959).

[9] Townsend, A. A., "The structure of the turbulent boundary-layer," Proc. Cambridge Phil. Soc. **47**, 375–395 (1951).

[10] Falkner, V. M., "The resistance of a smooth plate with turbulent boundary-layer," Aircraft Engr. **15**, 65–69 (March 1943).

[11] Schulz-Grunow, F., "New frictional resistance law for smooth plates," NACA TM 986 (1941).

[12] Goldschmied, F. R., "Theory of incompressible turbulent skin-friction and prediction of turbulent separation," Goodyear Aircraft Corp. GER 5388 (May 1953).

[13] Goldschmied, F. R., "Preliminary checkout data obtained in the 6″ × 60″ boundary-layer channel @ 0″ WG and 25″ WG suction," NACA Lewis Flight Propulsion Lab. (1951); unpublished. Note: The 6″ × 60″ channel is described in Ref. 16.

[14] Dhawan, S., "Direct measurements of skin-friction," NACA TN 2567 (1952).

[15] Smith, D. W. and Walker, J. H., "Skin-friction measurements in incompressible flow," NACA TN 4231 (1958).

[16] Sandborn, V. A., "Preliminary experimental investigation of low-speed turbulent boundary-layers in adverse pressure gradients," NACA TN 3031 (1953).

[17] Newman, B. G., "Some contributions to the study of the turbulent boundary-layer near separation," Australian Aeronautical Research Committee Rept. ACA-53 (March 1951).

[18] Robertson, J. M., "Prediction of turbulent boundary-layer separation," J. Aeronaut. Sci. **24**, 631–632 (1957).

[19] Donaldson, C. duP. and Lange, R. H., "Study of the pressure rise across shock-waves required to separate laminar and turbulent boundary-layers," NACA TN 2770 (1952).

[20] Goldschmied, F. G., "Skin-friction of incompressible turbulent boundary-layers under adverse pressure gradients," NACA TN 2431 (1951).